Positive Cross Correlations in a Three-Terminal Quantum Dot with Ferromagnetic Contacts

A. Cottet, W. Belzig, and C. Bruder

Department of Physics and Astronomy, University of Basel, Klingelbergstrasse 82, 4056 Basel, Switzerland

(Received 31 July 2003; published 19 May 2004)

We study current fluctuations in an interacting three-terminal quantum dot with ferromagnetic leads. For appropriately polarized contacts, the transport through the dot is governed by dynamical spin blockade, i.e., a spin-dependent bunching of tunneling events not present in the paramagnetic case. This leads, for instance, to positive zero-frequency cross correlations of the currents in the output leads even in the absence of spin accumulation on the dot. We include the influence of spin-flip scattering and identify favorable conditions for the experimental observation of this effect with respect to polarization of the contacts and tunneling rates.

DOI: 10.1103/PhysRevLett.92.206801 PACS numbers: 73.23.–b, 72.70.+m, 72.25.Rb

Quantum fluctuations of current in mesoscopic devices have attracted considerable attention in past years (for reviews, see Refs. [1,2]). It has been shown that the statistics of noninteracting fermions leads to a suppression of noise below the classical Poisson value [3–5] and to negative cross correlations in multiterminal structures [6]. This was recently confirmed experimentally in a Hanbury Brown–Twiss setup [7]. The question of the sign of cross correlations has triggered a lot of activity [8], and different mechanisms to obtain *positive* cross correlations in electronic systems have been proposed. Employing a superconductor as a source, positive cross correlations have been predicted for several setups [9]. This is because a superconducting source injects highly correlated electron pairs. Screening currents due to long-range Coulomb interactions lead to positive correlations in the finite-frequency voltage noise measured at two capacitors coupled to a coherent conductor [8,10]. Last, positive cross correlations can occur due to the correlated injection of electrons by a voltage probe [11], or due to correlated excitations in a Luttinger liquid [12].

Below, we will be interested in noise correlations in a quantum dot. This problem was addressed theoretically in the sequential-tunneling limit [13] and in the cotunneling regime [14]. Noise measurements [15] were in agreement with the Coulomb-blockade picture [13]. Cross correlations between particle currents in a paramagnetic multiterminal quantum dot were studied in Ref. [16], and they were found to be negative. The noise of a two-terminal quantum dot with ferromagnetic contacts was studied in the sequential-tunneling limit [17,18], and, interestingly, a super-Poissonian Fano factor was found.

In this Letter, we consider an interacting three-terminal quantum dot with ferromagnetic leads. The dot is operated as a beam splitter: One contact acts as source and the other two as drains. Our main finding is that sufficiently polarized contacts can lead to a dynamical spin blockade on the dot, i.e., a spin-dependent bunching of tunneling events not present in the paramagnetic case. A striking consequence of this spin blockade is the possibility of positive cross correlations in the absence of correlated injection. Surprisingly, spin accumulation on the dot is not necessary to observe this effect. Furthermore, the sign of cross correlations can be switched by reversing the magnetization of one contact. The effect is robust against spin flips on the dot as long as the spin-flip scattering rate is less than the tunneling rates.

The system we have in mind is a quantum dot connected to three ferromagnetic leads $i \in \{1, 2, 3\}$, through tunnel junctions with capacitances C_i and net spin-independent tunneling rates γ_i (inset of Fig. 1). A voltage bias V is applied to leads 1 and 3; lead 2 is connected to ground. At voltages and temperatures much lower than the intrinsic level spacing and the charging energy $e^2/2C$ of the dot ($C = \sum_i C_i$), only one energy level of the dot located at E_0 needs to be taken into account. In this situation, the dot can be either empty or occupied with one electron with spin $\sigma \in \{\uparrow, \downarrow\}$. In the following, we will measure energies from the Fermi level $E_F = 0$ of lead 2.

The collinear magnetic polarizations P_j of the leads are taken into account by using *spin-dependent* tunneling rates $\gamma_{j\sigma} = \gamma_j(1 + \sigma P_j)$, where $\sigma = \pm 1$ labels the electron spin (up/down). In a simple model, the spin dependence is a consequence of the different densities of states for majority and minority electrons [19]. The rate for an electron to tunnel on/off the dot ($\epsilon = \pm 1$) through junction j is then given by $\Gamma^{\epsilon}_{j\sigma} = \gamma_{j\sigma}/\{1 + \exp[\epsilon(E_0 - eV_j)/k_BT]\}$, where $V_1 = V_3 = -C_2V/C$, $V_2 = (C_1 + C_3)V/C$. On the dot, there can be spin-flip scattering, for instance, due to spin-orbit coupling or magnetic impurities. Here, we will assume that the on-site energy on the dot does not depend on spin. Hence, due to the detailed-balance rule, the spin-flip scattering rate γ_{sf} does not depend on spin.

In the sequential-tunneling limit $\hbar\gamma_{j\sigma} \ll k_BT$, electronic transport through the dot can be described by the master equation [13,18]:

$$\frac{d}{dt} p_{\psi}(t) = \sum_{\varphi} M_{\psi,\varphi} p_{\varphi}(t), \quad (1)$$

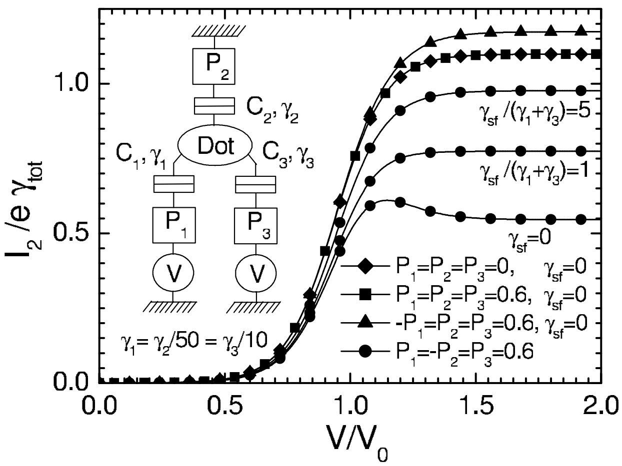

FIG. 1. Current-voltage characteristic of a quantum dot connected to three ferromagnetic leads $i \in \{1, 2, 3\}$, with respective polarizations P_i, through tunnel junctions with capacitances C_i and net tunneling rates γ_i (circuit shown in the inset). A bias voltage V is applied to leads 1 and 3; lead 2 is connected to ground. The average current I_2 through lead 2 is shown as a function of voltage, for $C_1 = C_2 = C_3$, $\gamma_1 = \gamma_2/50 = \gamma_3/10$, $k_BT/E_0 = 0.1$, and different values of lead polarizations. The current is plotted in units of $e\gamma_{\mathrm{tot}} = e\gamma_2(\gamma_1 + \gamma_3)/(\gamma_1 + \gamma_2 + \gamma_3)$; the voltage in units of $V_0 = E_0C/(C_1 + C_3)e$; E_0 is the position of the dot level. For $P_1 = P_2 = P_3$, I_2 coincides with the paramagnetic case (diamonds). In the other cases, the high-voltage limit of I_2 can be larger or smaller than the paramagnetic value, depending on the lead polarizations. For $P_1 = -P_2 = P_3 = 0.6$ (circles), the effect of spin-flip scattering is shown. Spin-flip scattering makes the $I_2 - V$ curve tend to the paramagnetic one.

where $p_\psi(t)$, $\psi \in \{\uparrow, \downarrow, 0\}$, is the instantaneous occupation probability of state ψ at time t, and

$$\hat{M} = \begin{bmatrix} -\Gamma_\uparrow^- - \gamma_{sf} & \gamma_{sf} & \Gamma_\uparrow^+ \\ \gamma_{sf} & -\Gamma_\downarrow^- - \gamma_{sf} & \Gamma_\downarrow^+ \\ \Gamma_\uparrow^- & \Gamma_\downarrow^- & -\Gamma_\uparrow^+ - \Gamma_\downarrow^+ \end{bmatrix} \quad (2)$$

depends on the total rates $\Gamma_\sigma^\epsilon = \sum_j \Gamma_{j\sigma}^\epsilon$ and $\gamma_\sigma = \sum_j \gamma_{j\sigma}$. The stationary occupation probabilities $\bar{p}_\psi$ are

$$\bar{p}_\sigma = \frac{\Gamma_\sigma^+\Gamma_{-\sigma}^- + \gamma_{sf}(\Gamma_\sigma^+ + \Gamma_{-\sigma}^+)}{\gamma_\sigma\gamma_{-\sigma} - \Gamma_\sigma^+\Gamma_{-\sigma}^+ + \gamma_{sf}\sum_{\sigma'}(\Gamma_{\sigma'}^+ + \gamma_{\sigma'})}, \quad (3)$$

and $\bar{p}_0 = 1 - \bar{p}_\uparrow - \bar{p}_\downarrow$. The average value $\langle I_j \rangle$ of the tunneling current $I_j(t)$ is $\langle I_j \rangle = e\sum_{\epsilon,\sigma}\epsilon\Gamma_{j\sigma}^\epsilon \bar{p}_{A(\sigma,-\epsilon)}$, where $A(\sigma, \epsilon)$ is the state of the dot after the tunneling of an electron with spin σ in the direction ϵ; i.e., $A(\sigma, -1) = 0$, $A(\sigma, +1) = \sigma$.

In the following, we consider $E_0 > 0$ (for $E_0 < 0$, see [20]). The voltage V will always be assumed to be positive, such that it is energetically more favorable for electrons to go from the input lead 2 to the output leads 1 or 3 than in the opposite direction. The typical voltage dependence of $I_2 \equiv \langle I_2 \rangle$ is shown in Fig. 1. The total current I_2 is exponentially suppressed at low voltages, increases around a voltage $V_0 = E_0C/(C_1 + C_3)e$, and saturates at higher voltages. The width of the increase is determined by k_BT/e. The high-voltage limit of I_2 depends on the polarizations P_i and rates γ_i but not on the capacitances C_i. For a sample with magnetic contacts, this limit can be higher or lower than that of the paramagnetic case, depending on the parameters considered. In the high-voltage limit, $I_2(P_1, P_2, P_3) - I_2(0, 0, 0) = 2e\gamma_c P_{\mathrm{out}}\langle S \rangle$, where $P_{\mathrm{out}} = (P_1\gamma_1 + P_3\gamma_3)/(\gamma_1 + \gamma_3)$ is the net output lead polarization, $\langle S \rangle = \nu(P_2 - P_{\mathrm{out}})$ is the average spin accumulation on the dot [21], and $\gamma_c = \gamma_2(\gamma_1 + \gamma_3)/(\gamma_1 + 2\gamma_2 + \gamma_3)$. Here, ν is a positive function of the polarizations, the tunneling, and scattering rates, which tends to 0 at large γ_{sf}. Having a saturation current different from the paramagnetic case requires $P_{\mathrm{out}} \neq 0$ and $\langle S \rangle \neq 0$. Spin-flip scattering modifies the $I_2 - V$ curve once γ_{sf} is of the order of the tunneling rates. It suppresses spin accumulation and makes the $I_2 - V$ curve tend to the paramagnetic one.

The power spectrum of tunneling current correlations in leads i and j is defined as $S_{ij}(\omega) = 2\int_{-\infty}^{+\infty} dt \exp(i\omega t)\langle \Delta I_i(t)\Delta I_j(0)\rangle$, where $\Delta I_i(t) = I_i(t) - \langle I_i \rangle$. The terms $\langle I_i(t)I_j(0)\rangle$ can be written as a function of the conditional probabilities $P_{\psi,\varphi}^c(t)$ which are the occupation probabilities of the state ψ at time t if at $t = 0$ the state was φ, and which are zero for $t < 0$. Solving Eq. (1) with the initial condition $P_{\psi,\varphi}^c(t = 0) = \delta_{\psi,\varphi}$ leads to $P_{\psi,\varphi}^c(t)$. The Fourier transform of $P_{\psi,\varphi}^c(t)$ is $\hat{P}^c(\omega) = \int_0^\infty dt \exp(i\omega t)\hat{P}^c(t) = -(i\omega + \hat{M})^{-1}$. The eigenvalues of the matrix $\hat{M}$ thus govern the frequency dependence of $\hat{P}^c(\omega)$. The nonzero eigenvalues are $\lambda_\pm = \frac{1}{2}(-2\gamma_{sf} - \gamma_\uparrow - \gamma_\downarrow \pm \Delta)$, with $\Delta^2 = 4\gamma_{sf}^2 + (\gamma_\uparrow - \gamma_\downarrow)^2 - 4\gamma_{sf}(\Gamma_\uparrow^+ + \Gamma_\downarrow^+) + 4\Gamma_\uparrow^+\Gamma_\downarrow^+$. This eventually leads to $S_{ij}(\omega) = \delta_{ij}S_j^{Sch} + \sum_{\sigma,\sigma'} S_{i,\sigma,j,\sigma'}^c(\omega)$, where $S_j^{\mathrm{Sch}} = 2e^2\sum_{\epsilon,\sigma}\Gamma_{j\sigma}^\epsilon \bar{p}_{A(-\epsilon,\sigma)}$ is the Schottky noise produced by tunneling through junction j, and

$$\frac{S_{i,\sigma,j,\sigma'}^c(\omega)}{2e^2} = \sum_{\epsilon,\epsilon'} \epsilon\epsilon'[\Gamma_{i\sigma}^{\epsilon'} G_{A(\sigma,-\epsilon'),A(\sigma',\epsilon)}(\omega)\Gamma_{j\sigma'}^\epsilon \bar{p}_{A(\sigma',-\epsilon)} + \Gamma_{j\sigma'}^{\epsilon'} G_{A(\sigma',-\epsilon'),A(\sigma,\epsilon)}(-\omega)\Gamma_{i\sigma}^\epsilon \bar{p}_{A(\sigma,-\epsilon)}]. \quad (4)$$

Here, we defined $G_{\psi,\varphi}(\omega) = P_{\psi,\varphi}^c(\omega) + \bar{p}_\psi/i\omega$. For frequencies larger than the cutoff frequencies $\lambda_\pm$, the spectrum $S_{ij}(\omega)$ tends to the uncorrelated spectrum $\delta_{ij}S_j^{\mathrm{Sch}}$. In the following, we will consider mainly the zero-frequency limit of $S_{ij}(\omega)$, because the frequencies $\lambda_\pm \sim \gamma_i$ are difficult to access in experiment. Note that at zero frequency the contribution of the screening currents ensuring electroneutrality of the capacitors after a tunneling event [8] is zero; i.e., $S_{ij} \equiv S_{ij}(0)$ is the signal measured in practice [22].

Figures 2 and 3 show the Fano factor $F = S_{22}/2eI_2$ and the cross correlations S_{13} as a function of V for $\gamma_{sf} = 0$.

Well below V_0, the current is due to thermally activated tunneling and the noise is Poissonian. At very low voltage, $eV \leq k_B T$, the crossover to thermal noise is observed. Around $V = V_0$, F and S_{13} show a step or a dip. The high-voltage limit strongly depends on tunneling rates and polarizations. In the paramagnetic case, the limit of F lies in the interval $[1/2, 1]$, and that of $S_{13}/2eI_2$ in $[-1/8, 0]$. In the ferromagnetic case, the high-voltage limit of F can be either sub-Poissonian or super-Poissonian, as already pointed out in the two-terminal case [17]. Spin accumulation is not a necessary condition for having a super-Poissonian Fano factor, as can be seen for $P_1 = P_2 = P_3$, where $\langle S \rangle = 0$. In this case, the essential point is that the current can flow only in short time windows where the dot is not blocked by a down spin (see the inset of Fig. 2). This dynamical spin blockade leads to a bunching of tunneling events, and explains the super-Poissonian Fano factor.

The cross correlations can be either positive or negative (see Fig. 3). Note that a super-Poissonian F does not necessarily imply positive cross correlations, as shown by the case $-P_1 = P_2 = P_3 = 0.6$ in Figs. 2 and 3, for which the cross correlations are even more negative than in the paramagnetic case. Indeed, relation (4) together with charge conservation imply that $S_{22} - S_2^{\mathrm{Sch}} = \sum_{\sigma,\sigma'} S^c_{1,\sigma,3,\sigma'}(\gamma_{1\sigma} + \gamma_{3\sigma})(\gamma_{1\sigma'} + \gamma_{3\sigma'})/\gamma_{1\sigma}\gamma_{3\sigma'}$ at $V \gg V_0$. Thus, at $V \gg V_0$, a super-Poissonian F is equivalent to positive cross correlations only if the two output leads have identical polarizations. For the case $-P_1 = P_2 = P_3 = 0.6$, cross correlations are negative in spite of the super-Poissonian F because the correlated electrons are mostly up electrons flowing through lead 3. Note that $\mathrm{Re}[S_{13}(\omega)]$ can change sign for intermediate frequencies and vanishes for $\omega \gg \lambda_\pm$ [20].

The effect of spin-flip scattering is shown in the inset of Fig. 3. Spin-flip scattering influences the cross correlations once γ_{sf} is of the order of the tunneling rates. In the high-γ_{sf} limit, cross correlations tend to the paramagnetic case for any value of the polarizations. Thus, strong elastic spin-flip scattering suppresses positive cross correlations, in contrast to what happens with inelastic scattering in [11]. In practice, experiments with a quantum dot connected to ferromagnetic leads and $\gamma_{sf} \ll \gamma_{\mathrm{tot}}$ have already been performed [23]. Thus, spin-flip scattering should not prevent the observation of positive cross correlations in quantum dots.

Finally, we address the problem of how to choose parameters that favor the observation of positive cross correlations. First, finite lead polarizations are necessary [16] (see the insets of Fig. 4). However, it is possible to get positive cross correlations even if $P_2 = 0$, provided the output leads 1,3 of the device are sufficiently polarized (dashed lines in the insets of Fig. 4). The case where the three electrodes are polarized in the same direction seems the most favorable. In the high-voltage limit, choosing $P_1 = P_2 = P_3$ and $\gamma_{sf} = 0$ leads to

$$S_{13} = \frac{16e^2\gamma_1\gamma_2^2\gamma_3[(\gamma_1 + 2\gamma_2 + \gamma_3)P_1^2 - \gamma_1 - \gamma_3]}{(\gamma_1 + \gamma_3)(\gamma_1 + 2\gamma_2 + \gamma_3)^3(1 - P_1^2)}. \quad (5)$$

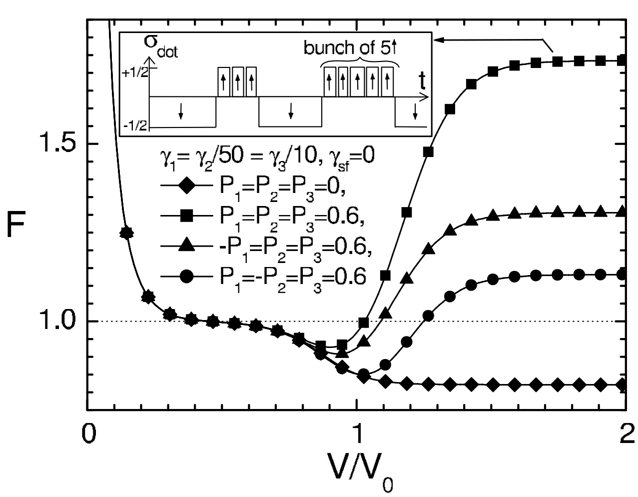

FIG. 2. Fano factor $F = S_{22}/2eI_2$ of lead 2 as a function of voltage, for the same circuit parameters as in Fig. 1. In all curves $\gamma_{sf} = 0$. For $P_1 = P_2 = P_3$, the Fano factor is different from that of the paramagnetic case (diamonds) in contrast to what happens for the average currents. The inset shows the typical time dependence of the spin on the dot, in the high-voltage limit $V \gg V_0$ for the case $P_1 = P_2 = P_3 = 0.6$.

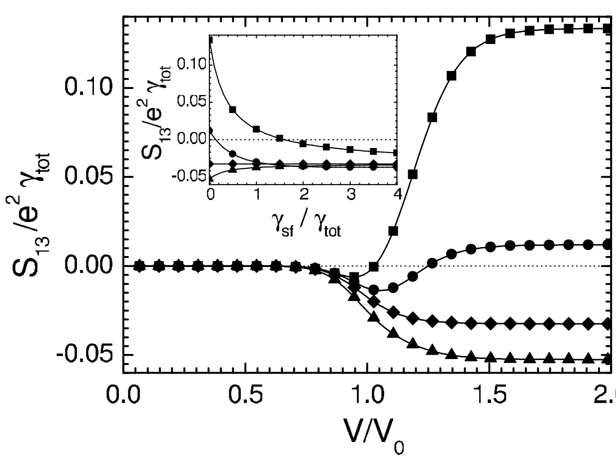

FIG. 3. Current cross correlations between leads 1 and 3 as a function of voltage. The curves are shown for the same circuit parameters as in Fig. 2. The cross correlations can be positive in the cases $P_1 = -P_2 = P_3 = 0.6$ (circles) and $P_1 = P_2 = P_3 = 0.6$ (squares). Note that the sign of cross correlations can be reversed by changing the sign of P_1. In all curves $\gamma_{sf} = 0$. The inset shows the influence of spin-flip scattering on the cross correlations in the high-voltage limit $V \gg V_0$. In the paramagnetic case (diamonds), spin-flip scattering has no effect. In the limit $\gamma_{sf} \gg \gamma_{\mathrm{tot}}$, the cross correlations tend to the paramagnetic value.

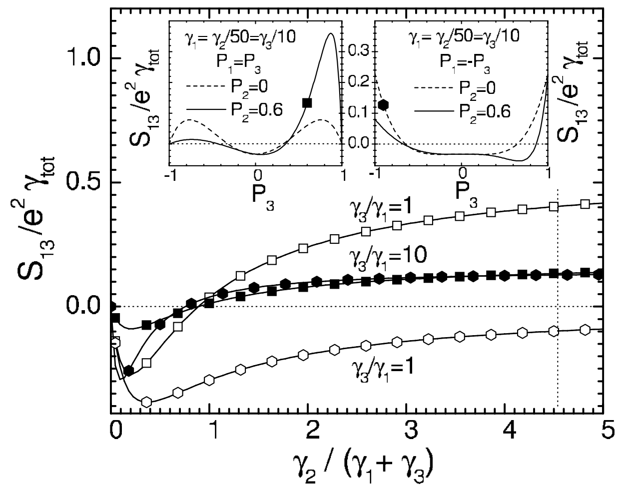

FIG. 4. Influence of the asymmetry between γ_2 and $\gamma_1+\gamma_3$ on the high-voltage limit of the cross correlations, for $P_1 = P_2 = P_3 = 0.6$ (squares) and $-P_1 = P_3 = 0.9$, $P_2 = 0$ (hexagons), for $\gamma_3/\gamma_1 = 10$ (full symbols) and $\gamma_3/\gamma_1 = 1$ (empty symbols). Large values of $\gamma_2/(\gamma_1+\gamma_3)$ favor positive cross correlations. For $-P_1 = P_3 = 0.9$, $P_2 = 0$, an asymmetry between γ_1 and γ_3 is also necessary. The vertical dotted line indicates the ratio $\gamma_2/(\gamma_1+\gamma_3)$ corresponding to Figs. 1 and 2. The two insets show the high-voltage limit of the cross correlations as a function of P_3, for $\gamma_1 = \gamma_2/50 = \gamma_3/10$, $P_1 = P_3$ (left inset), $P_1 = -P_3$ (right inset), and $P_2 = 0$ (dashed lines) or $P_2 = 0.6$ (full lines). For all curves $\gamma_{sf} = 0$.

The asymmetry between the tunneling rates γ_i has a strong influence on the cross correlations (see Fig. 4). Large values of $\gamma_2/(\gamma_1+\gamma_3)$ favor the observation of positive cross correlations [see, e.g., Eq. (5)] by decreasing $\bar{p}_0$. This allows one to extend the domains of positive cross correlations to smaller values of the polarizations, which is important because experimental contact materials are not fully polarized. For $\gamma_1 = \gamma_2/10 = \gamma_3$, the polarizations $P_1 = P_2 = P_3 = 0.4$ typical for Co [24] lead to positive cross correlations of the order of $S_{13}/e^2\gamma_{tot} \simeq 0.08$. With $\gamma_{tot} \simeq 5$ GHz, this corresponds to 10^{-29} A^2 s, a noise level accessible with present noise-amplification techniques [15].

In conclusion, we have demonstrated that transport through a multiterminal quantum dot with ferromagnetic leads is characterized by a new mechanism: dynamical spin blockade. As one of its consequences, we predict positive current cross correlations in the drain contacts without requiring the injection of correlated electron pairs. We have included spin-flip scattering on the dot and have shown that the effect persists as long as the spin-flip rate is less than the tunneling rates to the leads.

We thank T. Kontos and C. Schönenberger for discussions. This work was supported by the RTN Spintronics, the Swiss NSF, and the NCCR Nanoscience.

[1] Ya. M. Blanter and M. Büttiker, Phys. Rep. **336**, 1 (2000).
[2] *Quantum Noise in Mesoscopic Physics*, edited by Yu.V. Nazarov (Kluwer, Dordrecht, 2003).
[3] V. A. Khlus, Sov. Phys. JETP **66**, 1243 (1987).
[4] G. B. Lesovik, JETP Lett. **49**, 592 (1989).
[5] M. Büttiker, Phys. Rev. Lett. **65**, 2901 (1990).
[6] M. Büttiker, Phys. Rev. B **46**, 12 485 (1992).
[7] M. Henny *et al.*, Science **284**, 296 (1999); W. D. Oliver *et al.*, Science **284**, 299 (1999).
[8] See the article of M. Büttiker, in *Quantum Noise in Mesoscopic Physics* (Ref. [22]).
[9] T. Martin, Phys. Lett. A **220**, 137 (1996); M. P. Anantram and S. Datta, Phys. Rev. B **53**, 16 390 (1996); J. Torres and T. Martin, Eur. Phys. J. B **12**, 319 (1999); T. Gramespacher and M. Büttiker, Phys. Rev. B **61**, 8125 (2000); J. Torres *et al.*, *ibid.* **63**, 134517 (2001); J. Börlin *et al.*, Phys. Rev. Lett. **88**, 197001 (2002); P. Samuelsson and M. Büttiker, *ibid.* **89**, 046601 (2002); Phys. Rev. B **66**, 201306 (2002); F. Taddei and R. Fazio, *ibid.* **65**, 134522 (2002).
[10] A. M. Martin and M. Büttiker, Phys. Rev. Lett. **84**, 3386 (2000).
[11] C. Texier and M. Büttiker, Phys. Rev. B **62**, 7454 (2000).
[12] I. Safi *et al.*, Phys. Rev. Lett. **86**, 4628 (2001); A. Crepieux *et al.*, Phys. Rev. B **67**, 205408 (2003).
[13] A. N. Korotkov, Phys. Rev. B **49**, 10 381 (1994); S. Hershfield *et al.*, *ibid.* **47**, 1967 (1993); U. Hanke *et al.*, *ibid.* **48**, 17 209 (1993).
[14] D. Loss and E. V. Sukhorukhov, Phys. Rev. Lett. **84**, 1035 (2000); D.V. Averin, in *Macroscopic Quantum Coherence and Quantum Computing*, edited by D.V. Averin *et al.* (Kluwer, Dordrecht, 2001).
[15] H. Birk *et al.*, Phys. Rev. Lett. **75**, 1610 (1995).
[16] D. A. Bagrets and Yu.V. Nazarov, Phys. Rev. B **67**, 085316 (2003).
[17] B. R. Bulka *et al.*, Phys. Rev. B **60**, 12 246 (1999).
[18] B. R. Bulka, Phys. Rev. B **62**, 1186 (2000).
[19] M. Julliere, Phys. Lett. **54**, 225 (1975).
[20] A. Cottet *et al.*, cond-mat/0403507.
[21] J. Barnas and A. Fert, Phys. Rev. Lett. **80**, 1058 (1998); S. Takahashi and S. Maekawa, *ibid.* **80**, 1758 (1998); J. Barnaś and A. Fert, Europhys. Lett. **44**, 85 (1998); F. Guinea, Phys. Rev. B **58**, 9212 (1998); H. Imamura *et al.*, *ibid.* **59**, 6017 (1999); A. Brataas *et al.*, Eur. Phys. J. B **9**, 421 (1999); X. H. Wang and A. Brataas, Phys. Rev. Lett. **83**, 5138 (1999).
[22] The total current correlations, including screening currents, are $S_{ij}^{tot}(\omega) = \sum_{n,m}[\delta_{i,n} - (C_i/C)][\delta_{j,m} - (C_j/C)]S_{nm}(\omega)$.
[23] M. Deshmukh and D. C. Ralph, Phys. Rev. Lett. **89**, 266803 (2002).
[24] M. Soulen *et al.*, Science **282**, 85 (1998).